

Supporting Information

Improved charge separation and transport with L-aspartic acid derived carbon-doped g-C₃N₄ for efficient visible-light photocatalytic H₂ production

Ikram Ullah,^a Ning Qin,^a Pei Zhao,^{*a} Jing-Han Li,^b Shuai Chen,^b and An-Wu Xu^{*b}

^aSchool of Energy and Power Engineering, Shandong University, Jinan 250061, P. R. China.

^bDivision of Nanomaterials and Chemistry, Hefei National Research Center for Physical Sciences at the Microscale, University of Science and Technology of China, Hefei 230026, P. R. China.

*Corresponding Authors:

Pei Zhao; pei.zhao@sdu.edu.cn

An-Wu Xu; anwuxu@ustc.edu.cn

Experimental Part

Synthesis of Photocatalysts

For preparation of CCN-*X* photocatalysts, 10 g of urea and different amounts of L-aspartic acid were dissolved in a mixed solution of 35 mL ethanol and 5 mL deionized water. The solution was heated in a water bath at 80 °C with continuous aging to remove the solvent. The obtained dry powder was then placed in a covered alumina crucible and annealed at 550 °C for 2 hours in air with a ramp rate of 5 °C min⁻¹. After cooling to room temperature, CCN-*X* photocatalysts were obtained, where *X* represents the weight content of L-aspartic acid (*X* = 1, 4, 8, 12, and 16 mg). For a counterpart, pristine CN was synthesized by the calcination of 10 g urea under the same conditions, resulting in a light-yellow powder termed as CN.

Characterization

TGA was conducted at NETZSCH TG 209 F1 Libra TGA analyzer with α -Al₂O₃ as the standard at a heating rate of 10 °C/min. XRD analysis was carried out employing a Rigaku TTR-III diffractometer (MXPAHF, Japan) with Cu K α radiation ($\lambda = 1.54178 \text{ \AA}$) under an operating voltage of 40 kV and a current of 200 mA. FTIR spectroscopy was performed on KBr pellet samples utilizing a Nicolet Nexus 8700 with a spectral range of 500–400 cm⁻¹. UV-Vis DRS of the samples were conducted using a Shimadzu 3700DUV spectrophotometer over a wavelength range of 200–800 nm with BaSO₄ as the reflectance reference. The spectra were converted to Tauc plots for calculating the optical bandgap through plotting $(\alpha h\nu)^2$ versus $h\nu$, where α indicates the absorption coefficient, h is Planck constant, and ν is frequency of light. TEM, SEM, and HAADF-STEM and its corresponding EDS images were recorded using H-7650 HITACHI transmission electron microscope, GeminiSEM 450, and FEI Talos F200X field emission high-

resolution transmission electron microscope operated at 200 kV, respectively. XPS and VB-XPS were measured using a Thermo ESCALAB 250Xi X-ray photoelectron spectrometer with monochromatized Al K α radiation as the excitation sources with a pass energy of 30 eV. EPR spectra of the samples were obtained employing a Bruker JEOL JES-FA200 ESR spectrometer with a microwave power of 1mW and a sweep width ranging from 314.5 to 334.5 mT. PL measurements were carried out on a JY Fluorolog-3-Tau fluorescence spectrophotometer with an excitation wavelength of 370 nm. TRPL measurements were performed with LaserStrobe time-resolved spectrofluorometer (Photon Technology International (Canada) Inc.) using a USHIO xenon lamp and a 914-photomultiplier detection technique. Multipoint Brunauer-Emmett-Teller (BET) method was employed to achieve specific surface areas of the samples.

Photoelectrochemical Tests

Photoelectrochemical measurements tests, including transient photocurrent response (TPR) and electrochemical impedance spectroscopy (EIS) were performed in a conventional three-electrode cell utilizing a CHI 760 electrochemical analyzer (Chenhua, Shanghai, China). The system consisted of Ag⁺/AgCl reference electrode, a Pt wire counter electrode, and an ITO glass working electrode. An aqueous solution of 0.5 M Na₂SO₄ was used as the electrolyte with a 300 W xenon lamp as the light source. The working electrode was prepared by dispersing 1 mL of ethanol and 10 μ L Nafion solution via sonication. Then, 100 μ L of the solution was drop-cast onto an ITO glass with an expose area of \approx 1 cm² and followed by drying in a microwave oven at 80 °C for 2 hours. The TPR of the photocatalysts were measured employing an on/off switch method with a bias voltage of 0.5 V under visible-light illumination, while EIS Nyquist curves were achieved at a bias voltage of -0.2 V under continuous irradiation.

Photocatalytic H₂ Evolution Tests

Photocatalytic H₂ production from water splitting was performed in a 500 mL Pyrex top-illumination reaction vessel equipped with a closed gas circulation and evacuation system (Perfect Light, Beijing, Labsolar-6A). In a conventional procedure, 50 mg of photocatalyst was dissolved in 100 mL aqueous solution containing 10 vol% TEOA. Subsequently, 1 wt% Pt was deposited onto the photocatalyst surface by photo deposition of H₂PtCl₆·6H₂O as a cocatalyst. The suspension was repeatedly evacuated to remove air and other gases before irradiation with a 300 W xenon lamp with a long-pass filter of ($\lambda \geq 420$ nm) as a visible-light source. The reaction solution was constantly aged, and the reaction temperature was maintained at 6 °C with a flow of cooling water during the photocatalytic reaction. H₂ evolution was measured by a gas chromatograph (GC1120, Shanghai Sunny Hengping Limited) utilizing a thermal conductivity detector and a 5 Å molecular sieve column with nitrogen as the carrier gas.

The AQE of CCN-8 photocatalyst with different monochromatic light illumination ($\lambda = 420, 450, 500, \text{ and } 550 \text{ nm} \pm 5\text{nm}$) was calculated by the following equation:

$$AQE = \frac{\text{Number of produced } H_2 \text{ molecules} \times 2}{\text{incident photons number}} \times 100\%$$

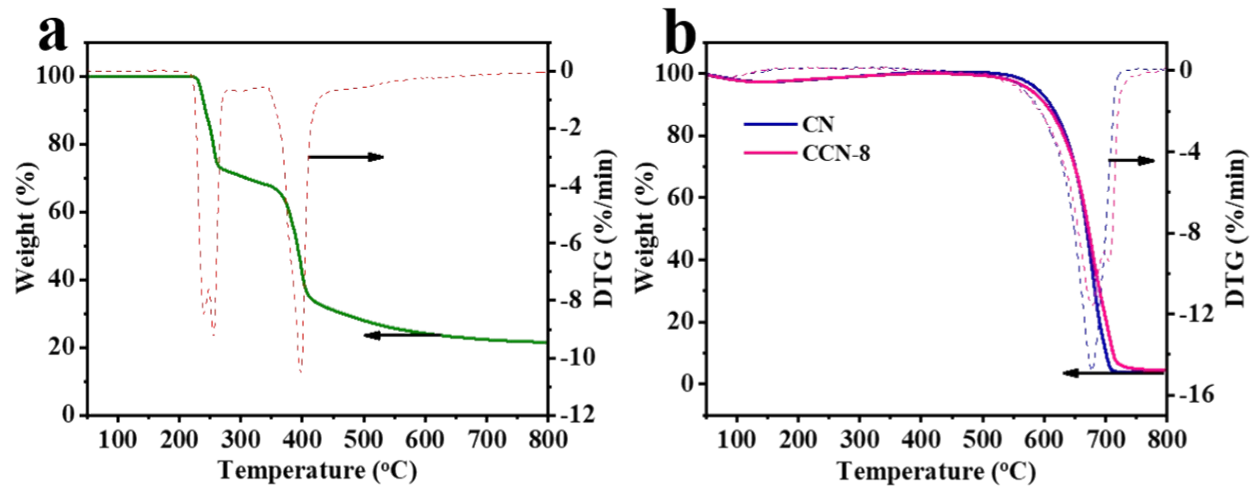


Figure S1. (a) TGA curve of LAA and (b) CN and CCN-8 photocatalysts with a rap rate of 10 °C min⁻¹.

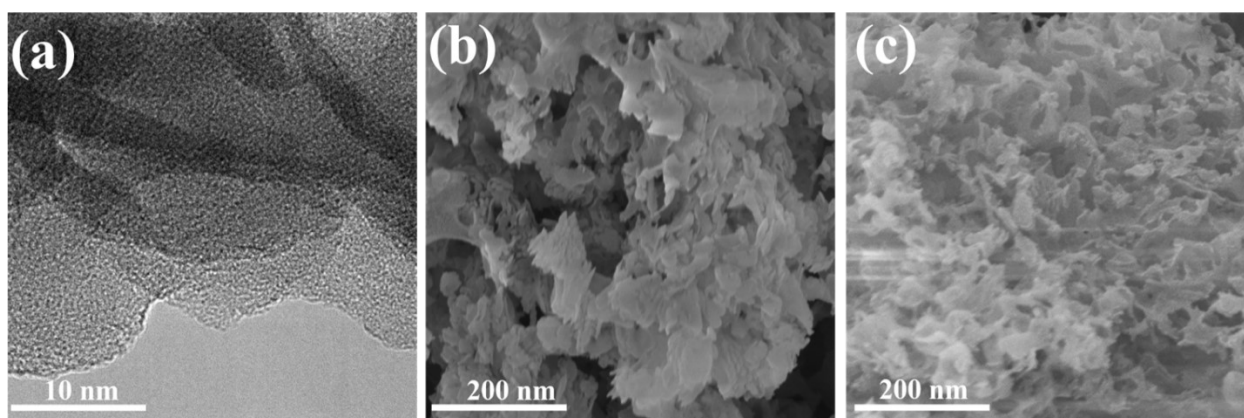


Figure S2. (a) HRTEM image of CCN-8 photocatalyst. The SEM images of (a) CN and (b) CCN-8 samples.

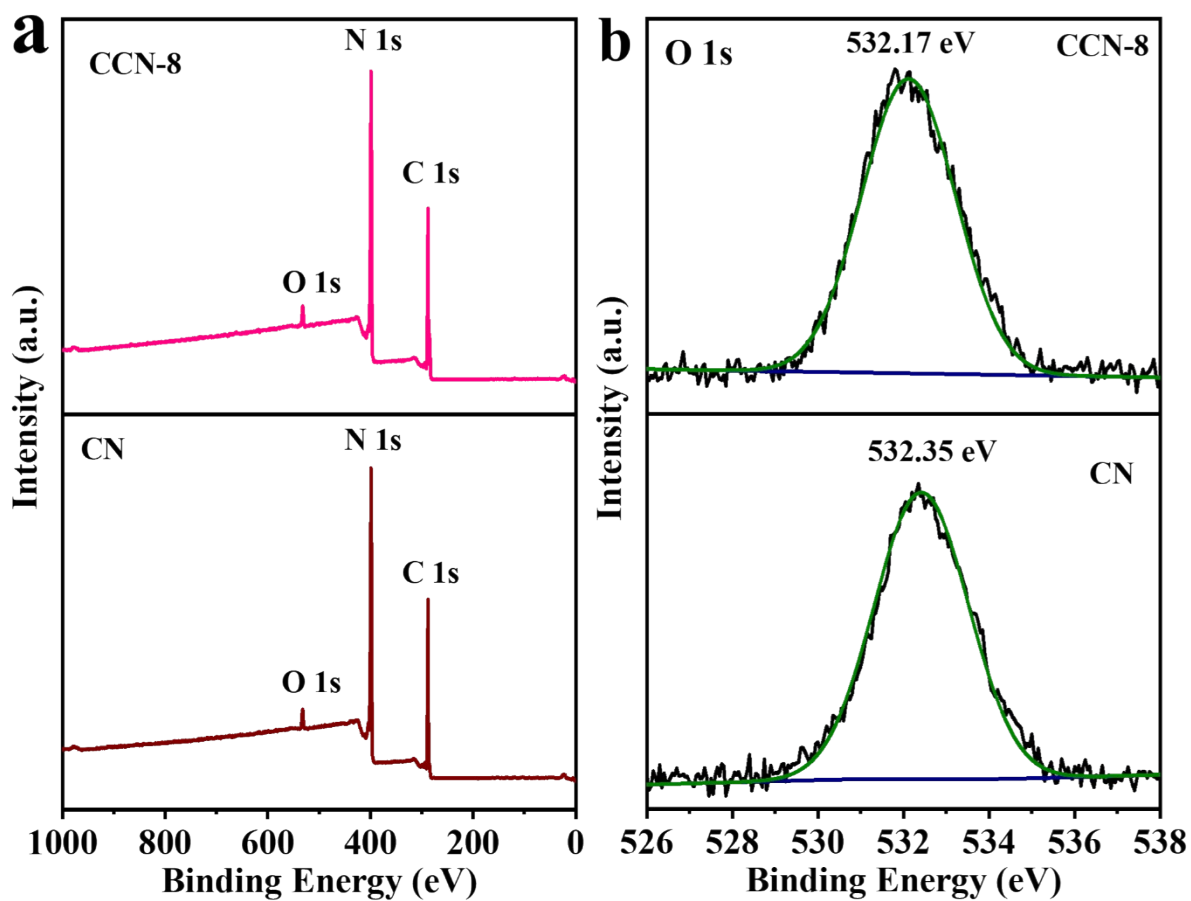


Figure S3. (a) XPS survey spectra and (b) high-resolution XPS spectra of O 1s for CN and CCN-8 samples.

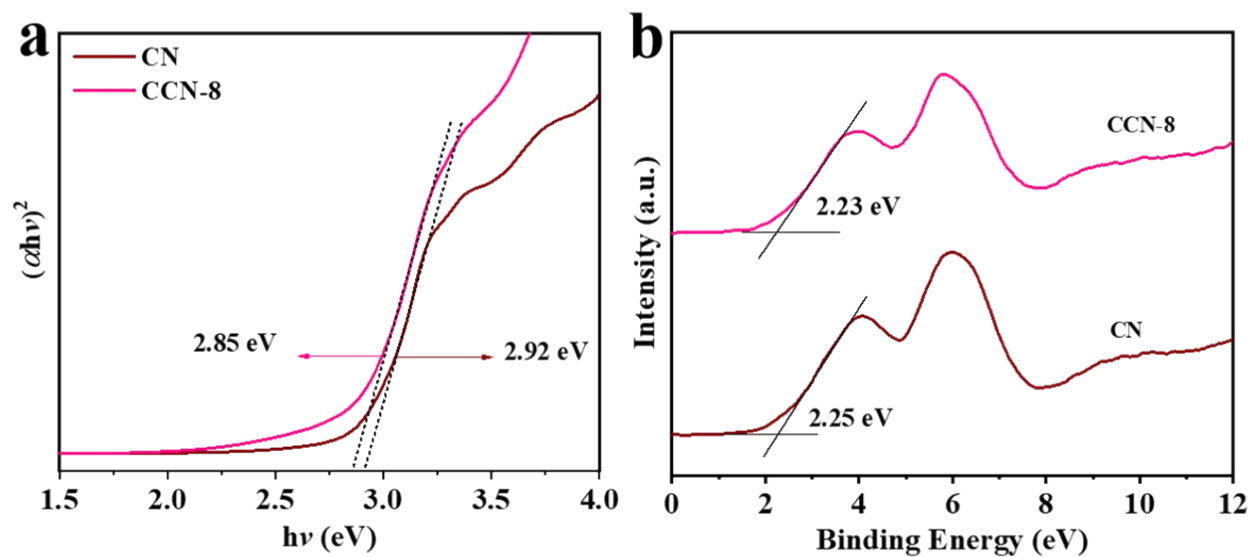


Figure S4. (a) Tauc curves and (b) VB-XPS spectra of CN and CCN-8 samples.

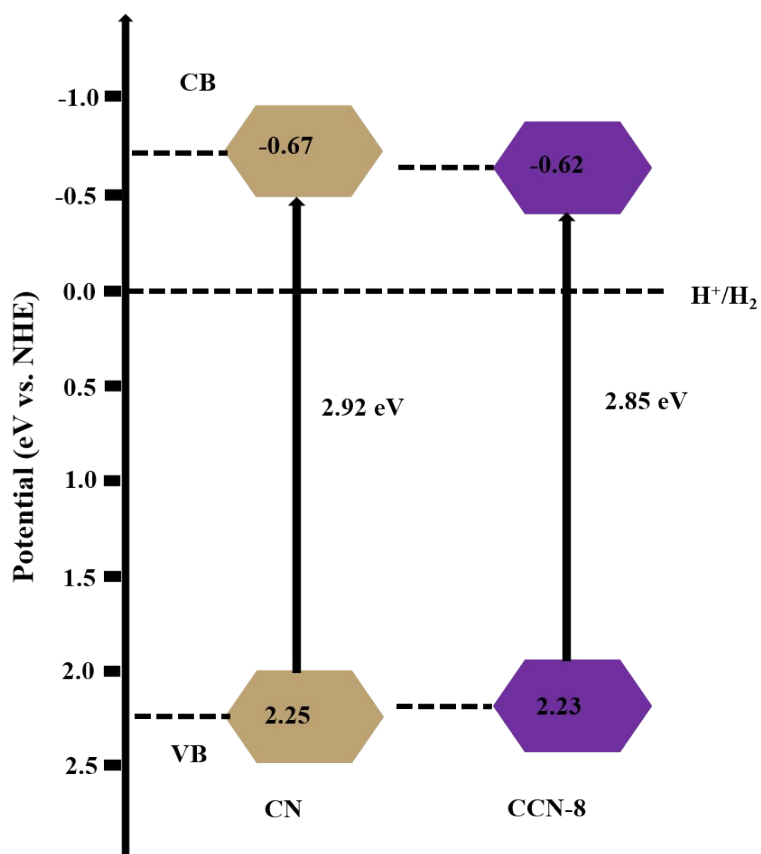


Figure S5. Electronic band configurations of CN and CCN-8 photocatalysts.

Table S1 Kinetics analysis of emission decay for CN and CCN-8 samples.

Photocatalysts	τ_1 (ns)	Rel (%)	τ_2 (ns)	Rel (%)	τ_3 (ns)	Rel (%)	τ (ns)	X^2
CN	2.68	45.77	12.83	34.32	0.54	19.99	1.78	1.19
CCN-8	1.56	43.39	7.05	27.18	0.31	29.43	0.79	1.23

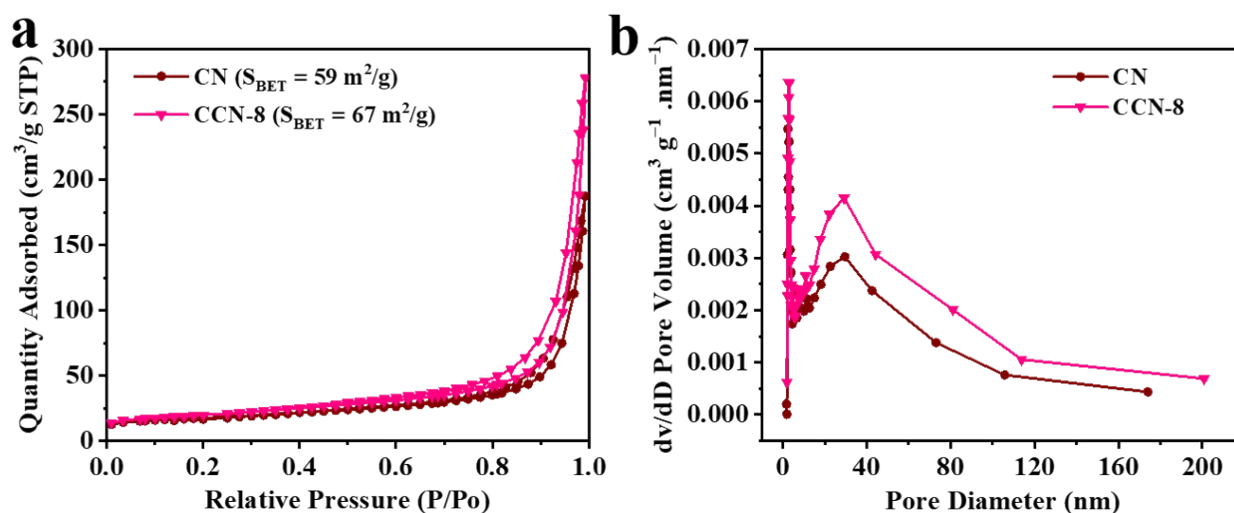


Figure S6. (a) Nitrogen adsorption/desorption isotherms and (b) pore size distribution curves of CN and CCN-8 photocatalysts.

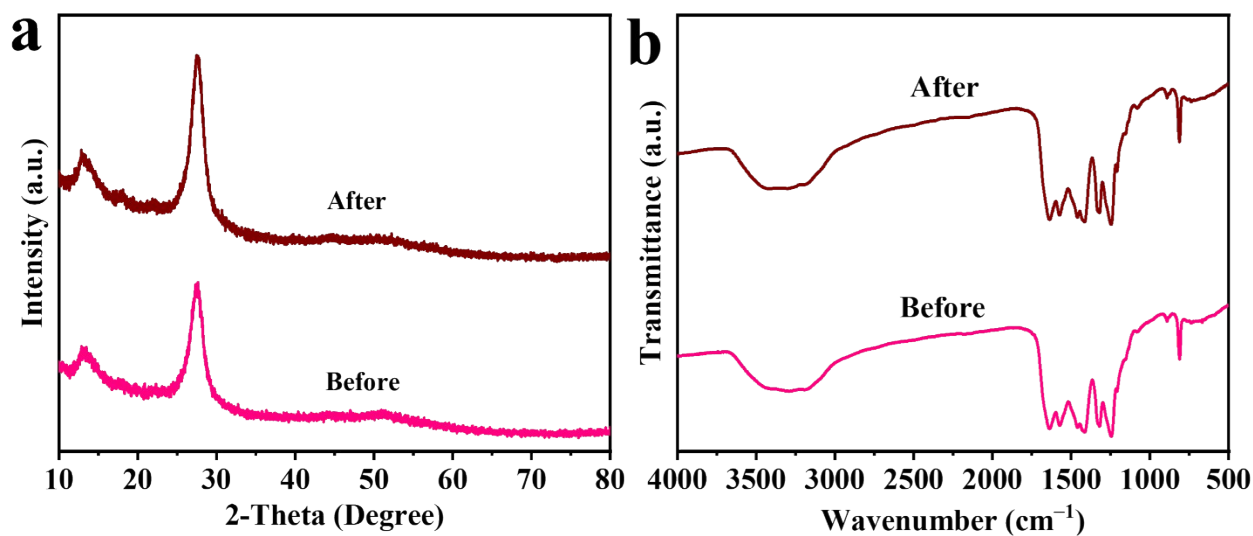


Figure S7. (a) XRD patterns and (b) FTIR spectra of CCN-8 before and after stability test.